Hydrogen adsorption on an open metal surface: H_2/Pd(210)

Markus Lischka and Axel Groß

Physik-Department T30, Technische Universität München, D-85747 Garching, Germany

(Received 27 August 2001; published 1 February 2002)

We present self-consistent density-functional calculations of the adsorption of atomic and molecular hydrogen on the (210) surface of palladium using a plane-wave basis set with optimized ultrasoft pseudopotentials. The layer relaxations of the (210) surface and the preferred adsorption sites for atomic hydrogen adsorption are determined. Furthermore, we show that on the rather open Pd(210) surface a molecular H_2 adsorption state becomes stabilized by the presence of atomic hydrogen on the surface. This provides a consistent explanation of recent experiments. An analysis of the bonding situation in terms of the local density of states is also presented.

I. INTRODUCTION

In the surface science approach, the study of the interaction of molecules with surfaces has traditionally concentrated on well-defined low-index surfaces. In particular, the interaction of hydrogen with metal surfaces has served as a model system for the investigation of fundamental reaction steps at surfaces, both experimentally[1–5] as well as theoretically.[5–13] However, imperfections of the surface, such as steps, are widely known to have a profound influence on adsorption and reaction processes.[14,15] For example, the surfaces of technologically relevant catalysts are very defect rich, and these defects are often assumed to be the active sites in heterogeneous catalysis. One way of closing this so-called "structure gap" between surface science and applied heterogeneous catalysis is to carry out experimental and theoretical studies on well-defined structured or defective surfaces. By this approach, the influence of a particular defect structure on the surface reactivity can be thoroughly studied.

In this paper, we report a theoretical study of the interaction of hydrogen atoms and molecules with the Pd(210) surface which was motivated by recent experiments on this system.[16,17] A preliminary account of this theoretical work has already been published.[17] We will show that the results of this theoretical study together with the experimental information lead to an unambiguous microscopic determination of the role of the steps in the hydrogen adsorption process at the Pd(210) surface.

The (210) surface is a relatively open surface that can be regarded as a stepped surface with a high density of steps. The geometry of this surface is shown in Fig. 1. Vicinal fcc (n10) surfaces have (100) terraces with steps running along the [001] direction and forming open (110)-like microfacets. This specific structure leads to unique properties of the hydrogen adsorption, as will be illustrated below.

Usually hydrogen adsorbs dissociatively at metal surfaces.[1] While at noble metals the dissociation is hindered by a sizable energy barrier, it occurs spontaneously on most transition metals, as, e.g., on palladium. Only at very low temperatures below 20 K, very weakly bound molecular adsorption states can be trapped in shallow physisorption wells.[18,19] On the other hand, reports of molecular chemisorption of H_2 are rare and restricted to stepped surfaces: On Ni(510), a molecular adsorption state at surface temperatures

up to 125 K has been observed at the step sites, but only after the surface was passivated with a dense atomic hydrogen layer.[20] On Cu(510), a weakly bound species has been observed at low temperatures on the pure surface.[21,22]

Recent experiments[16,17] have identified three atomic and two molecular adsorption states below 100 K on Pd(210). As the adsorption of hydrogen on this surface does not lead to any superstructure in low-energy electron diffraction (LEED) experiments, it is experimentally very difficult to identify the exact location and nature of the hydrogen adsorption states. In order to obtain this microscopic information, we have performed density-functional theory (DFT) calculations within the generalized gradient approximation (GGA).

The outline of this paper is as follows. In the next section we briefly summarize the computational details involved in our density-functional theory approach. We then present layer relaxation results for the Pd(210) surface in Sec. III A. In the main part of this paper, we discuss the DFT results for
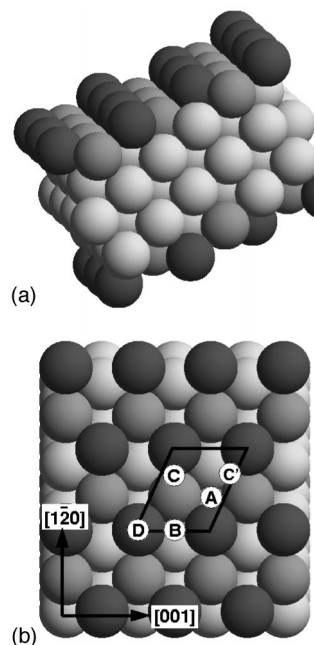

FIG. 1. Side and top view of the (210) surface. In the lower panel the surface unit cell and the adsorption site labels are included.

TABLE I. Layer relaxations of the Pd(210) surface. The DFT-GGA relaxations were computed for the pure Pd(210) surface, Pd(210) with one monolayer of hydrogen adsorbed, as well as Pd(210) with half a monolayer of subsurface hydrogen (in the octahedral position). The relative change to the bulk interlayer distance (in %) is given in parentheses. Positive numbers correspond to a surface expansion away from the bulk substrate.

Interlayer distance	Theory			Experiment	
	Pd(210)	Pd(210)/H($\theta = 1$)	Pd(210)/H($\theta_s = \frac{1}{2}$)	Pd(210) (Ref. 23)	Pt(210) (Ref. 24)
d_{12} [Å]	0.730 (-17)	0.791 (-11)	0.816 (-8)	0.84±0.04 (-3 ± 6)	(-23 ± 4)
d_{23} [Å]	0.854 (-3)	0.859 (-3)	0.856 (-3)	0.93±0.04 ($+7\pm5$)	(-12 ± 5)
d_{34} [Å]	0.976 ($+10$)	0.966 ($+9$)	0.974 ($+10$)	0.90±0.04 ($+3\pm5$)	($+4\pm7$)
d_{45} [Å]	0.847 (-4)	0.860 (-3)	0.866 (-2)	0.86±0.04 (-1 ± 5)	(-3 ± 7)
d_{Bulk} [Å]	0.885	0.885	0.885	0.870	0.877

atomic (Sec. III B) and molecular (Sec. III C) hydrogen adsorption on Pd(210) and compare them to recent experimental results.

II. THEORETICAL METHOD

Ab initio density-functional theory calculations were used to determine all the structural, electronic, and energetic results presented in Sec. III. The Kohn-Sham equations were solved in a plane-wave basis set using the Vienna *ab initio* simulation package (VASP).[25,26] In all calculations, we employed the generalized gradient approximation (GGA) of Perdew and co-workers (PW91).[27]

For a (1×1) surface unit cell of Pd(210), we used a Monkhorst-Pack **k**-point set[28] of 7×7×1, corresponding to 16 **k** points in the irreducible Brillouin zone, together with a first-order Methfessel-Paxton smearing[29] of width $\sigma = 0.1$ eV. All reported total energies were extrapolated to $\sigma \rightarrow 0$ eV. Relaxation calculations were carried out with a conjugate-gradient minimization using the Hellman-Feynman forces computed at a larger **k**-point set of 11×11 ×1 (36 **k** points in the irreducible zone) to ensure full convergence of the forces. To model the surface, the slab super-cell approach with periodic boundary conditions was used:[30] The Pd(210) surface is described by periodic slabs of either 11 or 21 layers and a separating vacuum region of 11 Å as depicted in Fig. 1.

The description of the core electronic states using a plane-wave basis set would require a very large energy cutoff. To reduce the computational effort the electron-ion interaction is described by ultrasoft Vanderbilt pseudopotentials[31] as constructed by G. Kresse and J. Hafner.[32] It was thus sufficient to use an energy cutoff of 200 eV (14.7 Ry) to obtain converged total energies.

All calculations have been performed at the GGA equilibrium lattice constant of 3.96 Å which is slightly larger than the experimental value of 3.89 Å. The dissociation energy and the bonding length of the free H_2 molecule were determined to be 4.55 eV and 0.75 Å, respectively (experiment:[33] 4.75 eV and 0.74 Å). Zero-point energies are neglected throughout this paper.

III. RESULTS AND DISCUSSION

A. Layer relaxation of Pd(210)

The interlayer distances at open surfaces can change considerably compared to the bulk values. To determine the layer relaxations, an 11 layer slab was set up with the lower six slab layers fixed to their bulk truncated positions using the theoretical bulk lattice constant. The top five layers were allowed to relax until the absolute value of the forces on each atom was smaller than 0.02 eV/Å. We checked that the results were converged with respect to the slab thickness by repeating the calculations with a 21 layer slab where the upper ten layers were fully relaxed.

The optimized interlayer distances are given in Table I. The DFT results suggest that there is indeed a very pronounced layer contraction of the first layer (-17%) compensated by an outward relaxation of the third layer ($+10\%$). Lateral displacements along the $[1\bar{2}0]$ direction have been found to be very small: Only the first and third layer atoms exhibit a somewhat significant displacement by 0.04 and 0.05 Å, respectively.

In Table I, the calculated layer relaxations are compared to experimental low-energy electron diffraction (LEED) results for Pd(210).[23] The relative experimental values with respect to the bulk (210) layer spacing differ significantly from the calculations. One has to note, however, that the absolute discrepancies between experiment and theory are still rather small ($\lesssim 0.1$ Å). In fact, the experimentally determined layer relaxations are surprisingly small for such an open surface. This becomes evident when the experimental Pd(210) results are compared to the interlayer relaxations measured for Pt(210).[24] One would expect similar relaxations for Pd and Pt since they have the same number of valence electrons and an almost identical lattice constant. Still the measured Pd(210) results are considerably smaller than the Pt(210) results.

These experimental results for Pt(210) are in fact rather close to our calculated values for Pd(210). And indeed, Kolthoff *et al.*[23] speculated that residual hydrogen coverages during the LEED experiments which were estimated to be lower than a quarter monolayer might be responsible for the small Pd(210) relaxations measured in their experiment. We tested this suggestion by determining the relaxations for

hydrogen-covered Pd(210). As Table I shows, one monolayer of adsorbed hydrogen atoms leads to a reduction in the interlayer relaxations, but not enough to reproduce the experimental results. Therefore we also checked whether subsurface hydrogen can account for the observed discrepancies. And indeed, already half a monolayer of hydrogen in the octahedral subsurface positions reduces the first layer contraction considerably (cf. Table I), but the other layer relaxations remain almost unchanged. This is also true for a full monolayer of subsurface hydrogen that just expands the first to second layer distance further to almost its bulk truncated value. Overall, the effect of adsorbed or subsurface hydrogen resembles the findings on the (111), (100), and (110) surfaces of palladium.[34] Still we conclude from our calculations that subsurface hydrogen could be the cause for the small interlayer relaxations of Pd(210) observed in the experiment by Kolthoff *et al.*[23]

As far as our hydrogen adsorption results are concerned, the relaxed geometry as given in the first column of Table I was used in all adsorption calculations in order to start from a fully self-consistent setup. Although the energy decrease due to the layer relaxations for the pure surface is just 0.06 eV, it was found that adsorbate-induced surface relaxations cannot be neglected in contrast to close-packed Pd surfaces.[13] Due to the openness of the surface, a full relaxation led to a decrease in total energy between 0.15 and 0.24 eV. All final adsorption energies are thus reported for a force-free, fully relaxed geometry.

B. Atomic adsorption

Recent experiments[16] have identified three different hydrogen adsorption sites on Pd(210). As hydrogen adsorbs at high coordination sites on close-packed palladium surfaces, the species with the highest adsorption energy (β_3) was tentatively assigned to the site with the highest coordination, i.e., the site labeled A in Fig. 1 with a fourfold coordination. The weaker bound H species (β_2 and β_1) were assigned to B and C′, respectively (C′ is actually twofold degenerate due to the mirror symmetry along [1$\bar{2}$0]). At the low-index Pd surfaces the energetic ordering of the atomic hydrogen adsorption sites indeed follows such a coordination argument.

To verify this assumption, the DFT adsorption energies at the three adsorption sites were computed in a (1×1) surface unit cell corresponding to a coverage of one monolayer. The hydrogen atoms were adsorbed asymmetrically on just one side of the slab. Due to the large size of the unit cell (3.96 ×4.42 Å), the interaction between hydrogen adsorbed in adjacent cells is negligible. A comparison between theoretical adsorption energies and experimental ones derived from thermal desorption spectroscopy (TDS) is shown in Table II. To account for the rather large error of 0.2 eV in the DFT binding energy of the hydrogen molecule, adsorption energies with respect to both the numerical and experimental binding energy of H_2 are reported in Table II. It is found that the intuitive assignment based on local coordination is not valid on the (210) surface. Instead, the step site B is found to be the most attractive one. We note that site A, locally equivalent to a (100) hollow site, exhibits a very similar adsorption

TABLE II. Adsorption energies per atom for the different adsorption sites as a function of hydrogen coverage on Pd(210). The adsorption energies calculated with respect to the experimental binding energy of H_2 are given in parentheses. For $\theta > 1$, the atomic adsorption energies are defined as the energies for additional adsorption of one H atom per surface unit cell with respect to the H_2 molecule in the gas phase. The notation of the sites refers to Fig. 1.

Coverage	Site	E_{ad} [eV]		State
		Theory	Expt. (Ref. 16)	
	B	0.52 (0.42)	0.41	β_3
	C′	0.51 (0.41)		
$\theta = 1$	A	0.45 (0.35)		
	O_d	0.21 (0.11)	0.19	α
	T_d	0.15 (0.05)		
$\theta = 2$	B,A	0.40 (0.30)	0.33	β_2
$\theta = 3$	B,A,C	0.26 (0.16)	0.23	β_1

energy as reported for the (100) surfaces previously.[13,34] Subsurface hydrogen either in the octahedral (O_d) or tetrahedral position (T_d) has been found to be exothermic by 0.21 and 0.15 eV, respectively.

If a monolayer of hydrogen is already adsorbed at site B, the next most favorable adsorption site at a $\theta = 2$ coverage is site A with a slightly decreased adsorption energy of $E_{ad} = 0.40$ eV compared to the pure surface. At an even higher coverage of $\theta = 3$, repulsive forces between the hydrogen atoms become dominant and the distance between the preadsorbed hydrogen atoms at site B as well as site A and the third hydrogen atom is maximized so that the third hydrogen atoms actually moves away from site C′ to the bridge site C with a significantly reduced adsorption energy of $E_{ad} = 0.26$ eV. The results are summarized in Table II where the experimental TDS peaks[16] have been assigned according to the DFT adsorption energies.

The energetical ordering of the adsorption sites can be analyzed and understood in terms of their local reactivity. By projecting the Kohn-Sham wave functions to atomic orbitals (truncated to a sphere with radius $r_s = 1.55$ Å),[35] the layer-resolved local density of states (LDOS) as shown in Fig. 2 can be obtained. As proposed by Hammer and Nørskov,[36,37]
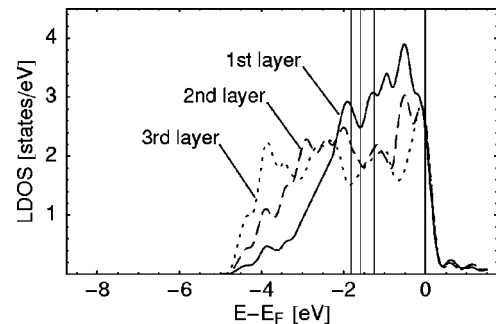

FIG. 2. Layer-resolved, local *d*-band density of states. Indicated by vertical lines are the Fermi level and the centers of the *d* bands. The third-layer LDOS is already very close to the bulk density of states of palladium.

the local reactivity is directly proportional to the distance of the d-band center to the Fermi level. Within this model, the interaction energy is approximately given by the perturbation expression,

$$\Delta\varepsilon \sim \frac{V^2}{|\varepsilon_d - \varepsilon_H|}, \quad V \ll |\varepsilon_d - \varepsilon_H|. \quad (1)$$

Assuming a constant filling of the d band and a constant coupling matrix V for different but similar configurations, it is only the distance $|\varepsilon_d - \varepsilon_H|$ that determines the energy gain due to a bond formation.

For bulk Pd, the d-band center is located 1.86 eV below the Fermi level. Going from bulk to the surface, the d-band center moves gradually higher in energy towards the Fermi level, i.e., the d-band center of the third-layer atom is still close to the bulk value at $\varepsilon_d = -1.80$ eV whereas for the second-layer atom we obtain $\varepsilon_d = -1.56$ eV and for the top atom $\varepsilon_d = -1.26$ eV. According to the Hammer-Nørskov model, it is thus the top Pd atom that is by far the most reactive one. To estimate the chemisorption potential energies at the actual adsorption sites A, B, and C', the geometrical average of the nearest-neighbor d-band centers[38] can be used. This indeed predicts the right ordering of the adsorption sites. The major origin of the variations in the bonding strength can thus be attributed to the local variations of the electronic structure at the surface.

C. Molecular adsorption

For hydrogen adsorption at temperatures below 100 K, two additional adsorption states were identified in TDS experiments.[17] These states were attributed to two molecular H_2 species as no mixing was found in H/D isotope exchange experiments. This is surprising as hydrogen dissociates spontaneously and without any activation barrier on $H_2/Pd(100)$ systems.[11,13]

In Figs. 3(a)–(c), three two-dimensional sections ("elbow plots") of the potential energy surface (PES) for the H_2 adsorption on Pd(210) are shown. These sections were computed using a 1×1 or a 2×1 surface unit cell where necessary and plotted by cubic interpolation of the total energies and Hellman-Feynman forces at more than 56 calculated points scanning different bond lengths of H_2, d, and the height of the center of mass above the surface, z. The slab Pd atoms were kept fixed at the positions of the relaxed pure slab. Only for the determination of the final adsorption geometry and energy was a full relaxation including the top five slab layers performed. These two-dimensional cuts are characterized as, e.g., B-A indicating that the section is given by the final atomic adsorption sites B and A (and the surface normal), or B-D-B indicating that the section is determined by two neighboring B sites with the molecule's center of mass fixed over the D site. The geometry of the hydrogen atoms is also shown by the insets in Figs. 3(a)–(c). The fixed orientation of the molecule is chosen according to the final adsorption geometry, i.e., for the B-A and A-C path the molecule is slightly tilted out of the plane parallel to the surface. The corresponding reaction path energies as a function of the surface distance z are depicted in Fig. 3(d). As can be seen
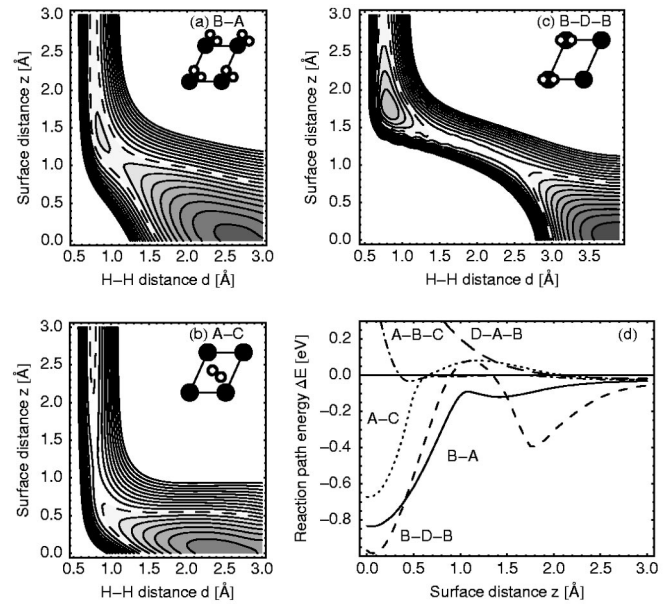

FIG. 3. (a)–(c) Two-dimensional sections through the PES for the dissociative adsorption of H_2 on Pd(210). The coordinates in the figure are the H_2 center-of-mass distance from the surface z and the H-H interatomic distance d. The molecular orientation is indicated in the insets. The contour spacing is 0.1 eV, and the vacuum energy level is marked by the dashed contour line. (d) Potential energy along the reaction paths for H_2 on Pd(210). The orientation of the H_2 molecule is fixed to the one of the corresponding two-dimensional PES.

clearly from Fig. 3(d), the H_2 molecule is first attracted towards the top Pd atom. Nevertheless, the DFT results suggests that at closer distances the H_2 molecule is able to dissociate spontaneously into the A and B sites as illustrated in Fig. 3(a). That the top site is most favorable at larger distances has also been found for other systems.[11,13,39] It is evident from Fig. 3 that no stable molecular adsorption state should exist at the clean Pd(210) surface due to the fact that hydrogen can always dissociate spontaneously.

This scenario is changed considerably by the presence of atomic hydrogen on the surface: In Fig. 4, the elbow plots and reaction path energies are shown for a surface precovered with a monolayer of hydrogen at site B. Dissociation along the B-A path is now obviously prohibited by the presence of atomic hydrogen at site B, but more important, the path to dissociation into the A and C sites is now blocked by a much more pronounced barrier of 220 meV. On the other hand, the attraction of the H_2 molecule to the top-layer Pd atom (site D in Fig. 1) is hardly influenced by the presence of the preadsorbed H atoms. The presence of hydrogen atoms thus leads to a metastable molecular adsorption state with a well depth of 270 meV. That the top site's reactivity is hardly influenced by the preadsorbed hydrogen atom can be traced back to the induced change in the local density of states (see Fig. 5): Although there is a resonance of the d band formed with the H 1s state at approximately -6.5 eV below the Fermi level (dashed line), the center of the d band just shifts from $\varepsilon_d = -1.26$ eV to $\varepsilon_d = -1.45$ eV. The top Pd atom is thus still more reactive than all other surface atoms.
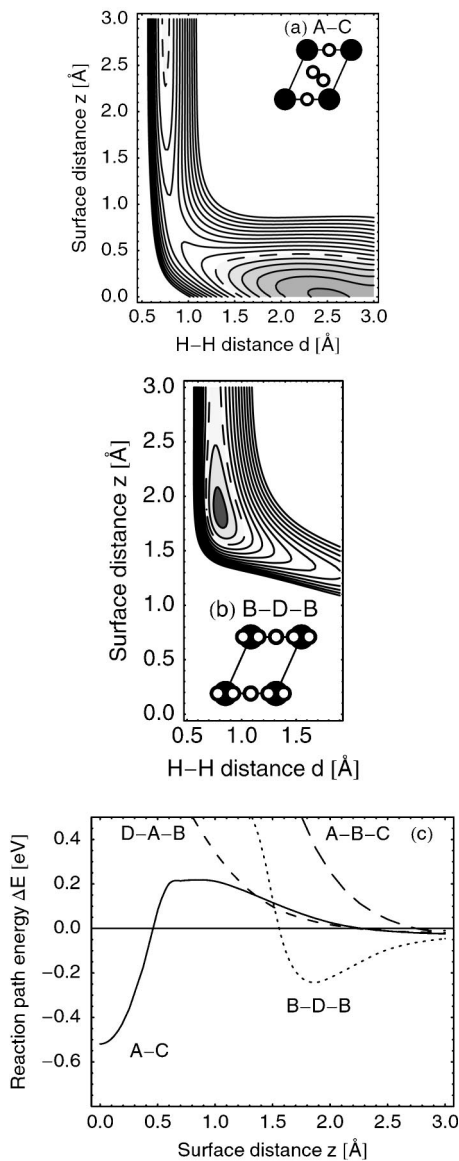
FIG. 4. (a) and (b) Two-dimensional sections through the PES for the dissociative adsorption of H_2 on Pd(210) precovered with a monolayer of hydrogen ($\theta=1$). (c) Potential energy along the reaction paths for H_2 on Pd(210) precovered with a monolayer of hydrogen ($\theta=1$). Cf. Fig. 3.

It is important to note that this is not just a site-blocking effect due to the hydrogen atom at site B. If the hydrogen atom is placed at the octahedral subsurface position instead, the same stabilization effect can be observed. Both B-A and A-C paths are then activated and the local minimum in the B-t-B section of the PES [Figs. 3(c) and 4(b)] corresponds to a true metastable molecular adsorption state. This stabilization can also be interpreted in terms of a bonding competition[40] between the preadsorbed hydrogen and the H_2 molecule lowering the adsorption energy and in turn increasing the dissociation barriers, due to the strong correlation of transition state energies and adsorption energies.[15,41]

To verify that the presence of atomic hydrogen indeed changes the dissociation channels from nonactivated to acti-
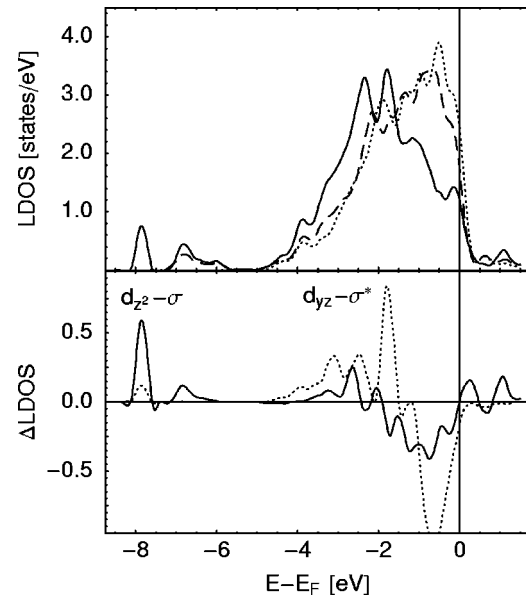

FIG. 5. Top panel: Local density of states of the top-most Pd atom before atomic hydrogen adsorption (dotted), after atomic hydrogen adsorption (dashed), and after additional adsorption of H_2 (solid line). Lower panel: Differences in orbital-resolved LDOS induced by H_2 adsorption on H/Pd(210) of the d_{z^2} (solid line) and the d_{yz} orbitals (dotted line).

vated, an "adiabatic" reaction path[13] was computed: Starting from an arbitrary but flat orientation far away from the surface over the most attractive site D, the H_2 molecule was fully relaxed within the four-dimensional subspace of a plane parallel to the surface, then pulled a little bit further towards the surface and relaxed again. By choosing different initial orientations we checked that the adiabatic reaction path does not depend on the initial conditions. This procedure mimics the discretized motion of a molecule with infinite mass and thus yields approximately the energetically most favorable reaction pathways. The reaction path energies for the pure (lower solid curve) and the H precovered surface (upper solid curve) are shown in Fig. 6. At large distances, the molecule is always steered towards the top Pd atom again, but then moves away to dissociate into the B and C′ sites on the pure surface. On the precovered surface, the H_2 molecule ends up in a local minimum in two adjacent C′ sites. The increase in the barrier height towards dissociation again demonstrates the stabilization of the molecular adsorption site above the top Pd atom.
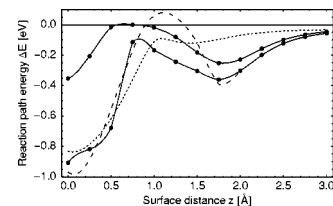

FIG. 6. Adiabatic reaction path energies for H_2 on the pure (lower solid curve) and the H pre-covered surface (upper solid curve). For comparison, the B-A (dotted) and B-D-B (dashed) reaction path energies are also shown.

TABLE III. Adsorption energies per molecule for the different adsorption configurations as a function of hydrogen coverage on Pd(210).

Coverage	Site	E_{ad} [eV]		State
		Theory	Exp. (Ref. 17)	
$\theta = 1$	D	0.27	0.25	γ_2
$\theta = 2$	D	0.22	0.16	γ_1
$\theta = 3$	D	0.09		δ

This molecular adsorption well at site D prevails even at higher atomic hydrogen coverages of $\theta = 2$ and 3. The adsorption energies for the fully relaxed geometries are 220 and 90 meV, respectively. We thus suggest that the two molecular adsorption species found in the TDS experiments[17] correspond to the molecular wells for two different local precoverages, $\theta = 1$ and $\theta = 2$. The two observed species thus do not populate different molecular adsorption sites, but just correspond to two different underlying atomic hydrogen coverages. Our findings are summarized in Table III.

Our interpretation is further confirmed by monitoring the work function change upon hydrogen adsorption: It was found in the experiment[16,17] that one monolayer of atomic hydrogen increases the work function by 120 meV whereas the work function decreases by 375 meV relative to the pure surface upon molecular hydrogen adsorption. To compute the work function change within the periodic plane-wave setup, an artificial dipole layer was introduced in the vacuum region[42] to account for the different vacuum potential energies on the pure and on the covered slab side. The difference in the vacuum levels exactly represents the induced work-function change. For a monolayer of atomic hydrogen, we find an increase of 250 meV. Molecular hydrogen on the other hand leads to a decrease of approximately 700 meV almost independent of hydrogen precoverage ($\theta = 0,1,2$). Although the absolute numbers are somewhat larger than the experimentally observed work-function change, the qualitative behavior is clearly reproduced.

The pronounced effect of the adsorbed molecule on the work function can also be inferred from the charge rearrangement as shown in Fig. 7. The strong hybridization between the H_2 molecule sitting 1.7 Å above the surface and the top Pd atom is visible in the electron-density contour plot of Fig. 7(a) and more clearly in the electron-density difference plot of Fig. 7(b). The electron-density difference is computed as the difference of the electron densities of the interacting system and the isolated H_2 molecule as well as the H-covered Pd(210) surface. It is evident that the H_2 molecule becomes strongly polarized upon adsorption and thus leads to a decrease of the work function.

Furthermore, the proposed scenario is corroborated by the experimentally observed vibrational frequency of the adsorbed H_2 molecule, $\hbar \omega_{vib} = 420$ meV. The theoretical vibrational frequency of the molecule at site D is computed to be 422 meV in the harmonic approximation (free H_2: 546 meV). The H-H molecular bond is thus slightly weakened indicating a population of the antibonding σ^* orbital. This picture is confirmed by analyzing the induced change of the
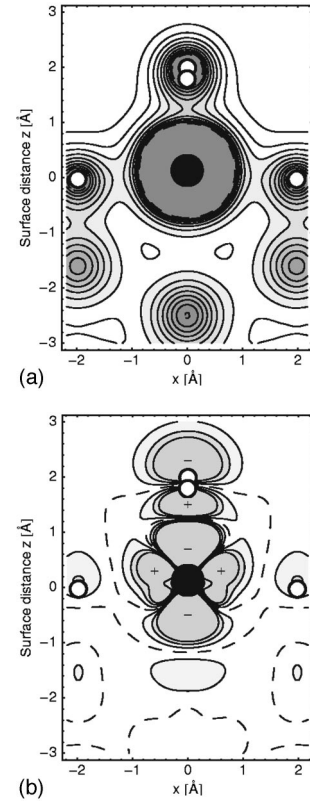

FIG. 7. (a) Electron-density contour plot of the molecular adsorption state in the x-z plane ($x \parallel [001]$). The positions of the H atoms and the top Pd atom are marked by open and filled circles, respectively. The top Pd atom and the H atoms at site B are exactly located within the plane, whereas the H atoms of the molecule are actually residing above and below the drawn plan. (b) Corresponding electron density difference plot. Regions of reduced electron density (i.e., positively charged) compared to the isolated systems H_2 and H/Pd(210) are marked with a minus sign, regions of enhanced electron density with a plus sign.

local density of states[43] as shown in Fig. 5. In the upper panel, the local density of states before (dashed) and after H_2 adsorption (solid) is depicted. A pronounced resonance peak at -8 eV is clearly visible. This resonance peak can be traced back to the interaction of the H_2 σ orbital with the Pd d_{z^2} band as illustrated by the induced change in the d_{z^2}-resolved LDOS (solid curve in the lower panel). Furthermore, the H_2 σ^* orbital shows a resonance peak with the d_{yz} band at -2 eV below the Fermi level and thus gets populated. Due to the symmetry of the minimum-energy configuration, there is no interaction with the d_{xz} band. The following interaction picture can thus be derived: When approaching over the top site, the H_2 molecule interacts with the d_{z^2}, d_{yz}, and d_{xz} orbitals of the top Pd atoms. By symmetry arguments, the H_2 σ orbital can only interact with the d_{z^2} orbital leading to a very small charge loss in the d_{z^2} band. On the other hand, the interaction of the antisymmetric H_2 σ^* orbital with the d_{yz} (d_{xz}) orbital gives rise to a filled $d_{yz} - \sigma^*$ resonance level yielding a net energy gain. Overall, the H-H bond is weakened and the H-Pd bond strengthened. A very similar scenario was also found for H_2 on Ni.[39]

As discussed in Ref. 17, the following scenario for H_2 adsorption on Pd(210) is thus suggested: On clean Pd(210), hydrogen adsorbs dissociatively. Once atomic hydrogen is present on the Pd(210) surface, further hydrogen dissociation becomes kinetically hindered close to the adsorbed hydrogen atoms although atomic adsorption sites are still available. This can be regarded as a local self-poisoning of hydrogen dissociation. In contrast to experimental results for H_2 adsorption on Ni(510),[20] where all adsorption sites for dissociative adsorption are occupied, or H_2 on Cu(510),[21,22] where step sites are occupied by the H_2 molecules on the pure surface, this local self-poisoning is essential to stabilize the molecular adsorption state on Pd(210) according to our DFT results. Nevertheless, this molecular adsorption state shows similar characteristics as the H_2/Cu(510) system discussed by Bengtsson *et al.*[22] with respect to the azimuthal anisotropy of the molecular state. Even with H preadsorbed at site B ($\theta = 1$) and at a full monolayer coverage of H_2, i.e., with every top site populated, the H_2 molecule is still able to rotate almost freely around its azimuthal angle. The maximum variation of the potential energy for an azimuthal rotation of the molecule by $\pi/2$ is just 4 meV. It should thus exhibit the same two-dimensional rotor states as found for the system H_2/Cu(510).

It is interesting to analyze why the Pd(210) surface has such unique features with respect to hydrogen adsorption. Since the steps at the (210) surface represent (110)-like microfacets, a Pd(110) surface might show similar properties. The site B at the Pd(210) surface (see Fig. 1) corresponds to the so-called long-bridge position at the (110) surface. However, on the Pd(110) surface the most favorable site for atomic adsorption of hydrogen is the pseudothreefold site on the micro-(111)-like facets[34] and not the long-bridge site. Furthermore, the top layer atoms are not protruding as much as on the Pd(210) surface which also modifies the local reactivity. Consequently, it is the combination of specific structural elements that enables the coexistence of atomic and molecular adsorption states on Pd(210). Other stepped surfaces might have similar specific properties. By studying structured surfaces in more detail one might discover specific sites with special chemical properties that can be useful for catalyzing certain reactions.

IV. CONCLUSION

We have presented DFT calculations for hydrogen adsorption on Pd(210). Layer relaxations of this open surface have been found to be significant. They are considerably reduced by the presence of hydrogen either on the surface or in subsurface positions. This suggests that the surprisingly small layer relaxations of Pd(210) found in the experiment might be caused by subsurface hydrogen which is hard to detect in the experiment.

We have examined and identified the hydrogen atomic adsorption sites for coverages of up to $\theta = 3$ per surface unit cell. It was found that the energetic ordering of the adsorption sites does not follow the simple coordination argument that the most favorable sites are those with the highest coordination of the adsorbate. Instead, the atom-surface bonds were analyzed within the Hammer-Nørskov d-band model. The lower coordination of the surface atoms at the kinked steps of the Pd(210) surface leads to a local d-band shift that correlates well with the hydrogen adsorption energies and thus accounts correctly for the high reactivity of the steplike top-layer Pd atom.

Furthermore, we have identified a molecular chemisorption state of H_2 on Pd(210) with a binding energy of 0.27 eV. Such states do not exist at flat metal surfaces. At Pd(210), the molecular state is stabilized by the presence of atomic hydrogen at the surface. A hydrogen precoverage is necessary as otherwise nonactivated pathways for dissociative hydrogen adsorption exists. Preadsorbed atomic hydrogen does not significantly disturb the interaction of the H_2 molecules with the Pd atoms as long as the H_2 molecules are further away from the surface, but it locally hinders the H_2 dissociation on Pd(210) although atomic adsorption sites are still available. Such unique features of structured surfaces might be useful for catalyzing certain reactions.

[1] K. Christmann, Surf. Sci. Rep. **9**, 1 (1988).

[2] K. D. Rendulic, G. Anger, and A. Winkler, Surf. Sci. **208**, 404 (1989).

[3] C. T. Rettner, D. J. Auerbach, and H. A. Michelsen, Phys. Rev. Lett. **68**, 1164 (1992).

[4] D. Wetzig, R. Dopheide, M. Rutkowski, R. David, and H. Zacharias, Phys. Rev. Lett. **76**, 463 (1996).

[5] D. Wetzig, M. Rutkowski, H. Zacharias, and A. Groß, Phys. Rev. B **63**, 205412 (2001).

[6] G. R. Darling and S. Holloway, Rep. Prog. Phys. **58**, 1595 (1995).

[7] A. Groß, Surf. Sci. Rep. **32**, 291 (1998).

[8] G.-J. Kroes, Prog. Surf. Sci. **60**, 1 (1999).

[9] B. Hammer, M. Scheffler, K. W. Jacobsen, and J. K. Nørskov, Phys. Rev. Lett. **73**, 1400 (1994).

[10] A. Gross, S. Wilke, and M. Scheffler, Phys. Rev. Lett. **75**, 2718 (1995).

[11] S. Wilke and M. Scheffler, Phys. Rev. B **53**, 4926 (1996).

[12] A. Gross and M. Scheffler, Phys. Rev. B **57**, 2493 (1998).

[13] A. Eichler, G. Kresse, and J. Hafner, Surf. Sci. **397**, 116 (1998).

[14] B. Hammer, O. H. Nielsen, and J. K. Nørskov, Catal. Lett. **46**, 31 (1997).

[15] B. Hammer, Phys. Rev. Lett. **83**, 3681 (1999).

[16] U. Muschiol, P. K. Schmidt, and K. Christmann, Surf. Sci. **395**, 182 (1998).

[17] P. K. Schmidt, K. Christmann, G. Kresse, J. Hafner, M. Lischka, and A. Groß, Phys. Rev. Lett. **87**, 096103 (2001).

[18] P. Avouris, D. Schmeisser, and J. E. Demuth, Phys. Rev. Lett. **48**, 199 (1982).

[19] S. Andersson and J. Harris, Phys. Rev. Lett. **48**, 545 (1982).

[20] A.-S. Mårtensson, C. Nyberg, and S. Andersson, Phys. Rev. Lett. **57**, 2045 (1986).

[21] K. Svensson, L. Bengtsson, J. Bellman, M. Hassel, M. Persson, and S. Andersson, Phys. Rev. Lett. **83**, 124 (1999).

[22] L. Bengtsson, K. Svensson, M. Hassel, J. Bellman, M. Persson, and S. Andersson, Phys. Rev. B **61**, 16 921 (2000).

[23] D. Kolthoff, H. Pfnür, A. G. Fedorus, V. Koval, and A. G. Naumovets, Surf. Sci. **439**, 224 (1999).

[24] X.-G. Zhang, M. A. Van Hove, G. A. Somorjai, P. J. Rous, D. Tobin, A. Gonis, J. M. MacLaren, K. Heinz, M. Michl, and H. Lindner, *et al.*, Phys. Rev. Lett. **67**, 1298 (1991).

[25] G. Kresse and J. Furthmüller, Phys. Rev. B **54**, 11 169 (1996).

[26] G. Kresse and J. Furthmüller, Comput. Mater. Sci. **6**, 15 (1996).

[27] J. P. Perdew, J. A. Chevary, S. H. Vosko, K. A. Jackson, M. R. Pederson, D. J. Singh, and C. Fiolhais, Phys. Rev. B **46**, 6671 (1992).

[28] H. J. Monkhorst and J. D. Pack, Phys. Rev. B **13**, 5188 (1976).

[29] M. Methfessel and A. T. Paxton, Phys. Rev. B **40**, 3616 (1989).

[30] M. C. Payne, M. P. Teter, D. C. Allan, T. A. Arias, and J. D. Joannopoulos, Rev. Mod. Phys. **64**, 1045 (1992).

[31] D. Vanderbilt, Phys. Rev. B **41**, 7892 (1990).

[32] G. Kresse and J. Hafner, J. Phys.: Condens. Matter **6**, 8245 (1994).

[33] G. Herzberg and K. P. Huber, *Molecular Spectra and Molecular Structure. IV. Constants of Diatomic Molecules* (Van Nostrand Reinhold, 1979).

[34] W. Dong, V. Ledentu, P. Sautet, A. Eichler, and J. Hafner, Surf. Sci. **411**, 123 (1998).

[35] A. Eichler, J. Hafner, J. Furthmüller, and G. Kresse, Surf. Sci. **346**, 300 (1996).

[36] B. Hammer and J. K. Nørskov, Nature (London) **376**, 238 (1995).

[37] B. Hammer, and J. K. Nørskov, Surf. Sci. **343**, 211 (2000).

[38] B. Hammer, Surf. Sci. **459**, 323 (2000).

[39] G. Kresse, Phys. Rev. B **62**, 8295 (2000).

[40] A. Alavi, P. Hu, T. Deutsch, P. L. Silvestrelli, and J. Hutter, Phys. Rev. Lett. **80**, 3650 (1998).

[41] Z.-P. Liu and P. Hu, J. Chem. Phys. **114**, 8244 (2001).

[42] J. Neugebauer and M. Scheffler, Phys. Rev. B **46**, 16 067 (1992).

[43] B. Hammer and M. Scheffler, Phys. Rev. Lett. **74**, 3487 (1995).